ACS Chemical Neuroscience

Article

Altered Processing of Beta-amyloid in SH-SY5Y cells induced by Model Senescent Microglia.

Dafina Martinova Angelova, and David Ronald Brown

ACS Chem. Neurosci., **Just Accepted Manuscript** • DOI: 10.1021/acschemneuro.8b00334 • Publication Date (Web): 27 Jul 2018

ACS Publications

is published by the American Chemical Society. 1155 Sixteenth Street N.W., Washington, DC 20036

Altered Processing of Beta-amyloid in SH-SY5Y cells induced by Model Senescent Microglia.

Dafina M. Angelova and David R. Brown*

Department of Biology and Biochemistry, University of Bath, Bath, UK.

Short Title: microglia and beta-amyloid

*Author for Correspondence:

Professor David R. Brown,

Department of Biology and Biochemistry

University of Bath

Claverton Down

Bath, BA2 7AY

United Kingdom.

Phone: +44-1225-383133

Fax: +44 -1225-386779

email: bssdrb@bath.ac.uk

ABSTRACT

The single greatest risk factor for neurodegenerative diseases is aging. Aging of cells such as microglia in the nervous system has an impact not only on the ability of those cells to function but also on cells they interact with. We have developed a model microglia system that recapitulates the dystrophic/senescent phenotype and we have combined this with the study of β-amyloid processing. The model is based on the observation that aged microglia have increased iron content. By overloading a human microglial cell line with iron we were able to change the secretory profile of the microglia. When combining these senescent microglia with SH-SY5Y cells we noted an increase in extracellular β-amyloid. The increased levels of β-amyloid were due to a decrease in the release of insulin-degrading enzyme by the model senescent microglia. Further analysis revealed that the senescent microglia showed both decreased autophagy and increased ER stress. These studies demonstrate the potential impact of an aging microglial population in terms of β-amyloid produced by neurons which could play a causal role in diseases like Alzheimer's disease. Our results also further develop the potential utility of an *in vitro* model of senescent microglia for the study of brain aging and neurodegenerative disease.

Key words: beta-amyloid, APP, microglia, ER stress, autophagy, insulin degrading enzyme

INTRODUCTION

There is overwhelming evidence for the importance of aging to the aetiology of neurodegenerative diseases[1]. Conditions like Alzheimer's disease (AD) increase in frequency as we age [2]. There are numerous diseases, including inherited forms of AD and prion diseases where dominant inherited mutations lead to neurodegeneration, but only when the carrier passes a certain age [3, 4]. Clearly understanding how the brain changes with age and how such changes result in the development of diseases involving neuronal dysfunction and loss is essential for understanding neurodegeneration. Therefore it is quite surprising that very few studies incorporate any aspect of the aging brain in their models. There is an inherent difficulty in including an aspect of aging in the development of a model of neurodegeneration because of the time requirement; eg. animal models would have to utilize animals that are towards the end of their life span [5]. *In vitro* models have even greater hurdles because such models are inherently short term [6, 7]. Therefore a potential alternative is to develop a method to induce a phenotypic change equivalent to that seen in cells from an aged brain.

Microglia are important cells in the brain that maintain neuronal well-being [8]. There is a plethora of information suggesting that microglia may participate in changes in the brain associated with neurodegenerative diseases [9-15]. These changes mostly relate to an altered secretory profile wherein the molecules released either result in reduced protection of neurons or an increase in proinflammatory or toxic molecules such as cytokines or reactive oxygen species [16]. Microglia change phenotype in this way with age and aged microglia are frequently described as dystrophic [17]. Microglia may develop a senescent-associated secretory phenotype (SASP) [18-20]. While SASP

is mostly associated with a study of molecular changes in cells, the dystrophic phenotype has largely been assigned on the basis of morphological changes. While both phenotypes are age associated they have been rarely used in conjunction to describe aged microglia. Understanding how microglia could enter such a phenotypic state and the potential of microglia to alter neuronal activity as a result is of considerable importance. Phenotypically, dystrophic microglia express increased levels of the iron storage protein ferritin [21, 22], which is a directly related to the increased levels of iron stored by them [23]. Increased iron levels in the brain are associated with both aging and patients with a variety of neurodegenerative diseases including AD and Parkinson's disease [24-27].

Dystrophic/senescent microglia are present in the brains of patients with AD [20, 28]. However, while their presence has been shown, any causative role is unknown. AD is mostly associated with the deposition of protein aggregates which include β-amyloid in the form of plaques and tau in the form of paired-helical filaments or tangles [29, 30]. Microglia secrete enzymes that are able to degrade beta-amyloid such as insulin-degrading enzyme (IDE) and neprilysin [31, 32]. There have also been reports suggesting neuronal loss in AD may come from activation of microglia as a result of interaction with beta-amyloid deposits [33, 34]. While there is considerable interest in microglia in terms of the pathology of AD, the impact of microglial senescence on the aetiology of the disease is unknown.

In this work we examine a new model of senescent microglia based on the observation that overloading microglia with iron forces them into a senescent-like phenotype. Combining these microglia with a neuronal cell line allowed us to

investigate how the change in phenotype alters the generation of β-amyloid. Following treatment of SH-SY5Y cells with conditioned medium from dystrophic microglia, there is an increase in β-amyloid present in the medium due to a decrease in the secretion of IDE. We have linked this change in IDE release to increased ER stress in microglia induced by the iron overload. The results cast light on the possible mechanism by which brain aging causes increased deposition of β-amyloid which could lead to AD.

RESULTS

Phenotype of iron-fed microglia

We used a human microglia cell line as the basis of our investigation. This line was chosen because it allowed the generation of sufficient cells for experiments and also because it maintained the species match for experiments involving β-amyloid generated by the human SH-SY5Y neuroblastoma cell line. As aged dystrophic microglia show high levels of stored iron we hypothesized that the dystrophic phenotype might be a consequence of high retention of iron [22]. Iron (particularly Fe(II)) causes damage to macromolecules and increased storage could be sufficient to induce changes seen in the dystrophic phenotype. For this reason we grew the human microglial cell line in 500 μM ferric ammonium citrate for at least two weeks.

In microglial cells grown in medium with high iron (iron-fed) we observed morphological changes similar to dystrophic microglia [17]. Under normal culture conditions (Figure 1A) microglia cells showed a small cell body with multiple projections and frequent ramification. In contrast iron-fed microglia (Figure 1B) showed no ramification and little to no projections. In many cases the microglia became amoeboid.

We verified that iron storage had occurred by three methods. First we used Perl's stain to identify iron deposits in the cells. As can be seen in Figure 2 control microglial cells (Figure 2A) had little to no deposits while iron-fed microglia showed large numbers of iron deposits in blue (Figure 2B). This demonstrates that iron-fed microglia store considerably more iron than the untreated control. Similarly, levels of ferritin are considered to reflect the levels of stored iron in cells. We measured the

levels of ferritin in control and iron-fed microglia by western blot and immune detection. The levels of ferritin in iron-fed microglia were much higher than in controls (Figure 2C and 2D). Lastly, we directly measured the levels of total iron in the microglia using a commercial kit. Iron-fed microglia showed considerably higher levels of total iron (Figure 2E).

Treatment of the microglial cell line with high concentrations of iron may have adversely affected their viability in culture. To control for this we measured their proliferation when compared to controls using a BrdU incorportation assay. Control and iron-fed human microglia were plated at a range of densities and the incorporation of BrdU assessed using an ELISA assay (Figure 3). Regardless of plating density, the iron-fed microglia showed no significant difference in BrdU incorporation suggesting that the iron-fed microglia maintained the same proliferation rate as the untreated controls.

Alteration in the secretory profile is an indication of a potential senescent phenotype in cells [35]. Microglia are known to show increased pro-inflammatory cytokine secretion with age [18]. Therefore we assessed a panel or cytokines associated with pro-inflammatory responses. Conditioned medium from control and iron-fed microglia were collected and normalized in relation to the protein content of the microglia used to conditioned the medium. The cytokines measured were IFN-γ, IL-10, IL-12p70, IL-13, IL-1β, IL-2, IL-4, IL-6, IL-8 and TNF-α (Table 1). Some of the cytokines tested could not be detected while other showed no changes. However, a number of the cytokines measured showed significant elevation. These included IL-1β, IL-6 and IL-8. The other measureable cytokines showed no changes (IL-2, IL10, IL13, TNFα).

This selective change in cytokines suggests a change in microglial phenotype similar to that suggested for aged microglia.

We also assessed other reported markers for aged/senescent microglia. It has been suggested that during the aging process microglia show reduced secretion of glutamate [36]. We used a commercial glutamate assay kit to measure glutamate released into culture by control and iron-fed microglia. Figure 4A shows that iron-fed microglia released significantly less glutamate than control microglia. In addition we measured two known markers for aged microglia. These included KV1.3 a microglial potassium channel and SIRT-1 (sirtuin-1) a deacetylase. KV1.3 has been shown to be altered in aged mice and to play a role in the release of cytokines [37, 38]. SIRT-1 has been shown to be decreased in aged microglia and this may contribute to cognitive decline and neurodegeneration [39].We used western blotting and specific antibodies to detect these proteins in extracts from control and iron fed microglia (Figure 4B-D). Iron-fed microglia showed a significant increase in the level of expression of KV1.3 but a significant decrease in expression of SIRT-1. These results are consistent with the suggestion that iron-fed microglia demonstrate a change in phenotype similar to dystrophic or senescent microglia *in vivo*. We are therefore confident that our iron-fed human microglia represent a robust *in vitro* model of senescent microglia.

Effect of Microglial Conditioned Medium on APP Metabolism in SH-SY5Y Neuronal Cells

Alzheimer's disease is associated with the deposition of abnormal proteins including β-amyloid. The rate of formation of β-amyloid depends upon the metabolism of its

precursor, APP and the relative activity of the two secretase pathways that either degrade APP to form β-amyloid (β-secretase dependent) or P3 (α-secretase dependent). In either pathway the end result is the release of an APP fragment by the gamma-secretase complex. However, the rate of formation of these products could be influenced by the level of expression of APP and the enzymes ADAM10 (α-secretase) and BACE-1 (β-secretase). The model we used to study the levels of these proteins was the human neuroblastoma cell line, SH-SY5Y. Conditioned medium was prepared from control and iron-fed microglia and applied to SH-SY5Y cells for 24 h. After that time the SH-SY5Y cells were assessed for the expression of these proteins by western blot and immunodetection with specific antibodies. As shown in Figure 5 treatment of SH-SY5Y cells with microglial conditioned medium had no significant effect on the expression of either APP or BACE-1. In contrast, conditioned medium from iron-fed microglia but not control microglia had a significant effect reducing the levels of ADAM10 protein by SH-SY5Y cells.

We investigated the consequences of altered ADAM10 expression through a variety of assays. First we used a dual luciferase assay of APP cleavage to assess if there is any change in the rate of formation of the AICD fragment of APP. In this system, a GAL4 DNA binding tag is attached to the C-terminal of the APP protein. The assay is dependent on the cleavage of this tagged form of APP and the release of the tag which is then able to induce luciferase expression by binding to the luciferase reporter. Our previous work has demonstrated that in SH-SY5Y cells, the predominant cleavage of this tagged APP is sequential via beta-secretase and then gamma secretase to release the tagged AICD fragment[40]. SH-SY5Y cells were transiently transfected with the APP expression plasmid, the luciferase reporter plasmid and a third *Renilla* luciferase construct that controls for transfection

efficiency and differences in cell number. The transfected cells were then treated with conditioned medium from control and iron-fed microglia for 24 h. Luciferase activity was then measured in extracts from the cells and compared to transfected controls that were treated only with serum free medium. The result showed that both medium from control and iron-fed microglia had a significant effect on the luciferase levels detected (Figure 6A). This suggests that AICD fragment formation is greatly reduced by microglia conditioned medium. However, there was no significant difference between control and iron fed conditioned medium. This implies that the change in ADAM10 expression induced by iron-fed microglia had no effect on rates of APP cleavage.

We then measured the activity of the ADAM10 promoter using a reporter construct containing the promoter for human ADAM10. The SH-SY5Y cells were similarly transiently transfected with this construct and the *Renilla* control. The transfected cells were then treated with conditioned medium from control and iron-fed microglia for 24 h. The result showed that neither medium from control nor iron-fed had any significant effect on the luciferase levels detected (Figure 6B). This implies that the change in ADAM10 protein expression we observed was not a consequence of altered transcription of ADAM10 mRNA.

Following from this we wished to confirm whether altered ADAM10 expression resulted in altered ADAM10 activity. We therefore used a FRET-based assay to assess ADAM10 activity in extracts of SH-SY5Y cells treated with conditioned medium from control and iron-fed microglia. The assay measured the cleavage of a tagged peptide substrate. After 24 h of treatment with conditioned medium extracts from the treated SH-SY5Y cells were applied to the assay and the level of cleavage measured. The results showed that there was no significant difference in ADAM10

activity in SH-SY5Y cells treated with conditioned medium from microglia (Figure 6C). The implication of this is that, despite the change in ADAM10 protein expression, there is no consequence of this in terms of measurable activity.

Lastly, as we have observed reduced protein expression of ADAM10 we looked for an alternative explanation for the change. It is known that ADAM10 translation can be down-regulated through the activity of the translation suppressor, FMRP (Fragile-x mental retardation protein)[41]. We assessed the expression of FMRP in SH-SY5Y cells by western blot. SH-SY5Y cells were treated with conditioned medium from control and iron-fed microglia for 24 h. Protein extracts were then prepared and the western blot procedure carried out. The levels of FMRP were assessed using a specific antibody. The results showed a significant increase in FMRP in SH-SY5Y cells treated with conditioned medium from iron-fed microglia but not from control microglia (Figure 6D & E). What this points to is that conditioned medium from iron-fed microglia increases the expression of the translation inhibitor FMRP known to regulate the translation of ADAM10.

The cleavage of APP causes release of β-amyloid from neuronal cells such as SH-SY5Y cells. The released β-amyloid can be detected in cell culture medium. We used a very sensitive MSD immunoassay to measure β-amyloid released into the serum free cell culture medium by SH-SY5Y cells. Treatment of SH-SY5Y cells with conditioned medium from control microglia for 24 h resulted in a large and significant reduction in β-amyloid (both $A\beta_{1-40}$ and $A\beta_{1-42}$) that could be detected in the medium (Figure 7A). In comparison SH-SY5Y cells treated with conditioned medium from iron-fed microglia had a significantly reduced effect on the levels of β-amyloid (Figure 7A-B). The implication of this result is that control microglia are more able to reduce the levels of β-amyloid released by SH-SY5Y cells than iron-fed microglia. It should

be noted that treatment of SH-SY5Y cells with just iron had no significant effect on β-amyloid levels (Suppl. Figure 1).

The decreased levels of β-amyloid detected in medium of SH-SY5Y cells following treatment with microglial conditioned medium can either be a result of decreased release of β-amyloid or increased breakdown of the peptide. While we have shown that conditioned medium from microglia reduced APP cleavage there was no significant difference between control and iron-fed microglia. Therefore the difference we noted in β-amyloid present in the medium is more likely to be a result of altered breakdown. We therefore used synthetic β-amyloid to measure its breakdown by microglia conditioned medium. Equal amounts of β-amyloid was placed in wells and treated with either serum free medium, control microglia conditioned medium or iron-fed microglia conditioned medium for 24 h. Following the assay, the levels of β-amyloid measured were compared as a percentage to the levels detected in the serum free medium control as a percentage. Three different concentrations of the conditioned medium were tested. β-amyloid (both $A\beta_{1-40}$ and $A\beta_{1-42}$) was degraded by the conditioned medium in direct relation to the amount of conditioned medium added (Figure 7C-D). At 25% and 50% concentrations conditioned medium from iron-fed microglia had a significantly weaker effect. The implication is that microglia release factors in their conditioned medium that degrade β-amyloid and iron-fed microglia release significantly less of these.

Microglia release a number of factors known to degrade β-amyloid. Among these are insulin-degrading enzyme (IDE)[42] and neprilysin[43]. We tested specific inhibitors of these enzymes to determine of the reduction in β-amyloid caused by microglial conditioned medium was due to the presence of these enzymes. We repeated the MSD assay for testing the degradation of β-amyloid by conditioned medium but

added either 30μM ML345 (IDE inhibitor) [44] or 10 μM thiorphan (neprilysin inhibitor) [45] in parallel. The results show that the IDE inhibitor but not the neprilysin inhibitor significantly reduced the degradation of β-amyloid (both $A\beta_{1-40}$ and $A\beta_{1-42}$) by microglia conditioned medium (Figure 7E-F). This implies that IDE is the likely candidate protein released from microglia that degrades β-amyloid in our system.

We verified that IDE was released by control and iron-fed microglia by collecting conditioned medium from microglia, concentrating it and testing for the presence of IDE by western blot. IDE was detected at equivalent expression levels in control and iron-fed microglia and was also present in the medium collected from the cells (Figure 7G-H). The levels of IDE in iron-fed microglial conditioned medium were significantly lower than for control. This supports the suggestion that iron-fed microglia release significantly less IDE than control microglia.

Mechanism of Reduced IDE Release by Iron-fed Microglia.

We observed no change in IDE expression in iron-fed microglia. Therefore, another factor must be altering the levels released. It has been reported that IDE released from microglia is influenced by changes in autophagy [46]. Therefore we assessed autophagic flux in our model microglia. The expression levels of the protein LC3-II are a reliable indicator of the level of autophagosomes in cells [47]. Inhibition of autophagy with bafilomycin in conjunction would then give an assessment of the turnover of LC3-II [48]. Therefore, an increase in LC3-II levels in microglia that remains unaltered by bafilomycin treatment would be indicative of reduced autophagy. Control and iron-fed microglia were grown in serum free medium and treated either with 13 nM bafilomycin or the equivalent volume of methanol vehicle (20 μL). After

16 h protein extracts were prepared from the cells and the levels of LC3-I and LC3-II determined by western blot (Figure 8). Iron-fed microglia grown in serum free medium showed significantly higher LC3-II levels than control microglia. Bafilomycin significantly increased the levels of LC3-II detected in control microglia when compared to the methanol control but there was no such change for iron-fed microglia with the same treatment. The results suggest that autophagy in iron-fed microglia is inhibited in comparison to control microglia.

Changes in autophagy are often associated with changes in endoplasmic reticulum (ER) stress. Mechanistically, this would provide a potential start point for the changes observed as ER stress can be induced by iron overload [49]. We therefore examined the expression of a range of proteins that either link or are associated with ER stress and autophagy. These include MTOR (mammalian target of rapamycin) associated with down-regulation of autophagy when phosphorylated [50], EIF2a (eukaryotic translation initiation factor 2a) associated with increased ER stress [51], SCAMP5 (secretory carrier membrane protein 5) which links increased ER stress to decreased autophagy [52], FMRP which decreases the expression of proteins such as SIRT1 as a result of ER stress [53], and acetylated NF-κB which is associated with alteration in released cytokines as a result of ER stress [54]. Extracts were prepared from control and iron-fed microglia and applied to the western blot procedure. Specific antibodies were used to detect bands associated with the proteins of interest (Figure 9) and the bands quantitated by densitometry (Table 2). There was a significant increase in the level of phosphorylated MTOR, but the levels of total protein remained the same. This change fits with the suggestion that autophagy is down regulated in iron-fed microglia. Similarly, levels of phosphorylated EIF2a were increased with no change in the total protein. This fits with the notion that ER stress

is increased in iron-fed microglia. Both FMRP and SCAMP5 were increased further supporting these suggestions. Lastly, acetylated NF-κB (p65) was increased with no change in total NF-κB levels. This change is also associated with decreased autophagy through decreased SIRT-1 activity [55].

As we have evidence that both autophagy and ER stress are altered in iron-fed microglia we wished to determine if inhibiting autophagy and inducing ER stress would cause a change in IDE release from control microglia. We therefore used bafilomycin to inhibit autophagy and both brefeldin A and tunicamycin to induce ER stress. Conditioned medium was collected from control microglia that had been treated overnight with these compounds and extracts were prepared from the treated microglia to assess cellular levels of IDE. The conditioned medium was concentrated, and the IDE levels were assessed by western blot (Figure 10). All three compounds significantly reduced the levels of IDE that could be detected in conditioned medium but had no effect on the cellular levels of IDE. These results support the notion that ER stress and consequential reduced autophagy cause reduced levels of IDE release by microglia.

Lastly, to verify that the effect of autophagy inhibition and ER stress diminish the ability of microglia to degrade β-amyloid, the conditioned medium from the microglia treated with bafilomycin, brefeldin A or tunicamycin was applied to the MSD assay using synthetic β-amyloid. β-amyloid was treated with the conditioned medium from the microglia for 24 h and the levels of β-amyloid remaining were assessed. Treatment of the microglia with all three compounds significantly decreased the degradation of β-amyloid (both $A\beta_{1-40}$ and $A\beta_{1-42}$), indicating that reduced IDE release resulted in decreased β-amyloid degradation (Figure 11).

DISCUSSION

Non-familial AD is the most common neurodegenerative disease and incidence rapidly increases with age, making the aging process the major risk factor [56]. Therefore, understanding how brain aging impacts the incidence of AD is a major necessity for its possible treatment. While the exact cause of AD remains unresolved, the deposition of aggregates of β-amyloid is at the least a significant marker for its progression and at the most the causative agent [57]. The true role of β-amyloid in the pathogenesis probably lies somewhere between these extremes. While the formation of β-amyloid is a normal cellular consequence of the metabolic breakdown of APP, increasing its levels either through alterations in the metabolic fate of APP or increasing its extracellular survival through reduced breakdown directly corresponds to increased possibility of extracellular aggregates forming [58-60].

There has been increasing discussion of the potential role of microglial aging and dysfunction in AD [20, 28, 61-63]. However, the nature of patient tissues and even animal models make assessment of molecular interactions difficult, necessitating cell models where real time interactions can be monitored and changes assessed. Our model of dystrophic/senescent microglia therefore provides an opportunity for which there is currently little alternative. Given the issues with rodent models to reproduce an inherently human disease [64] we deliberately chose human cell lines for our approach. While different microglia “states” such as activated and primed [65] or phenotypes such as ramified and phagocytic can be modelled, there are no such models for senescent/dystrophic microglia. The major criteria for determining the characteristics of dystrophic microglia is based on morphological changes in tissue which inherently poorly translates to *in vitro* models [18, 35]. Similarly, there is no universal marker that can discriminate a dystrophic microglia from any other [18].

Worse still is that large scale proteomics/transcriptomics based studies have failed to identify reproducible differences between aged microglia and controls, with each study listing almost incomparable data sets [66-71]. The one exception to this is ferritin expression. Microglia express more ferritin than most cells of the brain but this is further elevated in dystrophic microglia and implicates that iron storage is also increased [22]. A more objective way to assess senescence in microglia is to use the same criteria used for assessing general cellular senescence i.e. the characterization of their secretory phenotype [72]. The induction of the senescence associated secretory phenotype (SASP) is likely to become the standard approach to identify senescent cells in the absence of a specific marker [73].

We induced a senescent/dystrophic phenotype in microglia by iron overload. This resulted in a change in expression of ferritin and iron storage. While the high levels of iron used were artificial and unlikely to be encountered *in vivo*, they were employed as a means to an end and played no further role once we had induced the phenotype, as the high iron environment was removed from the culture system when analysing changes and producing conditioned medium. However, the levels of stored iron and the increase in ferritin levels we measured are in line with previous suggested increases in both iron concentrations and ferritin levels in specific brain regions that have previously been measured[74]. Of all the cell types in the brain, microglia show the largest increase in iron storage with age and are therefore likely to have much higher levels that the average for any specific brain region[25].

We verified the senescent/dystrophic phenotype by measuring molecules released by the microglia (cytokines and glutamate) [36, 75] as well as changes in protein

expression associated with an aged phenotype (KV1.3, SIRT-1) [37, 39]. Interestingly age associated changes in both KV1.3 and SIRT-1 have been shown to influence increased cytokine release [38, 39]. Other changes observed later in the study also support the SASP state of the iron-fed microglia. These include changes in autophagy and ER stress [76, 77].

The multitude of changes we have measured in our model microglia converge on a general phenotype that would be expected in a senescent cell. Along with altered release of molecules such as cytokines, these changes included reduced ability to deal with stress and a failure in processes aimed at clearing away damaged proteins such as autophagy.

The relation of microglia to AD has long been considered [78-81]. Similar to the study of many neurodegenerative diseases, the study of microglia in AD has principally concerned the physical relation of microglia in patient brains and transgenic mice to pathological hallmarks such as β-amyloid deposition [82] or neuronal loss [83]. The potential role of microglia has been suggested to be direct: causing neuronal loss through activation in response to β-amyloid [84], indirect: changing parameters such as plague load [85] or bystander: attracted to plaques without altering the pathology. There have been some suggestions that β-amyloid is not necessary to the mechanism of neuronal loss and that eliminating microglia in AD transgenic mice prevents neuronal loss without change to β-amyloid plaque levels [86]. However, the most convincing evidence suggests that microglia influence clearance of β-amyloid due to the production of enzymes able to degrade it or by phagocytic uptake [32]. Thus, regulation of β-amyloid clearance is the most likely physiological role of microglia in AD.

Our findings emphasize the importance of microglial proteases to the removal of β-amyloid and how disruption of the release of enzymes like IDE could compromise this role. The human microglia cell line we used released IDE which in our system almost completely removed β-amyloid released by SH-SY5Y cells over 24 h. IDE is released by primary microglia but not all microglia cell lines (e.g. BV2), indicating that caution must be used in the choice in cell lines to model age-related microglia changes [87, 88]. The reduced release in IDE we observed for iron-fed microglia was a result of reduced autophagy which has been previously observed [46, 89], but is a mechanism that has been poorly studied. It has been noted that changes in this pathway involve changes in the level of phosphorylated MTOR [89], which we also observed. Outside of the possible association of reduced IDE release with the dystrophic phenotype, we observed that both reduced autophagy and increased ER stress had the same effect. The implication is that any process that alters microglia in a similar way could also influence the levels of β-amyloid in the brain. However, reduced autophagy and increased ER stress are characteristics of senescence-associated secretory phenotype [76, 77]. It should also be noted that the change in IDE release was not due to a general failure in IDE expression in the cells as we did not observe any change in cellular expression.

There has been discussion of how important reduction in β-amyloid degrading enzymes is to AD. There are some reports that suggest that such a reduction would only contribute to late stage changes [90]. Of course, studies of patients don't take into account preclinical changes that may play a role in disease onset. The general consensus is that these enzymes are extremely important and regardless of causality, regulating their activity may have therapeutic value [91]. An additional consideration is the relative contributions of the different enzymes to β-amyloid

degradation in the brain. Our study has focused on IDE and not neprilysin because we found no contribution from the latter in our system, but this may not reflect the roles of these enzymes in AD. There has been suggestion that neprilysin is the main enzyme affected in AD [92] and others suggest it might be a different enzyme altogether, such as angiotensin-converting enzyme [93]. However, IDE is clearly important when considering β-amyloid degradation in the brain. First, IDE is reduced with age in regions associated with AD [94]. Second, overexpression of IDE causes a significant reduction in plaque load [95]. Thirdly given these enzymes are both released by microglia, and as the principal change may be in the SASP of microglia it may be a moot point exactly which enzyme is most involved.

A final additional factor is that enzymes generated by neurones themselves and released extracellularly might also contribute to APP degradation. Such enzymes include endothelin-converting enzyme and membrane type-metalomatrix proteins (MMPs)[96, 97]. These enzymes may also be released by SH-SY5Ys. Factors from microglia may also influence levels of these proteins which could have also affected levels of β-amyloid in our system.

We also examined other factors that could alter the generation of β-amyloid by SH-SY5Y cells. In particular we noted that conditioned medium from microglia significantly reduced the formation of AICD, a C-terminal cleavage product of APP, but this effect was replicated when the conditioned medium was generated from iron-fed microglia. While a change in the processing of APP could result in reduced release of β-amyloid by SH-SY5Y cells, and consequently the level of β-amyloid measured in the MSD assay, it has no bearing on the assays with synthetic β-amyloid. Therefore, these results support the potential role of microglia in regulating β-amyloid levels released from cells. Destruction of microglia in mice has been

shown to increase plaque size [98]. We also noted a significant change in the levels of ADAM10 expression in SH-SY5Y cells treated with conditioned medium from iron-fed microglia, but as there was no observed change in the activity of ADAM10, the consequences of this altered expression are likely to be insignificant to the processing of APP and the subsequent levels of β-amyloid. These findings do not rule out other potential changes to protein expression and metabolism in SH-SY5Y cells, but these may or may not have any bearing on APP metabolism specifically. While the study on microglia-neuron interactions is hardly new, there has been little study of the impact of microglia on APP processing in neurons. This is surprising given there is significant evidence that APP processing is influenced by cytokines released by microglia [99-101]. However, we are confident that a system of study such as ours will increase consideration of microglia in the study of APP.

In summary, we have established a unique model of senescent/dystrophic microglia and used this to examine the role of dystrophic microglia in the turnover of β-amyloid, a major player in AD. A comprehensive overview of our findings is illustrated in Figure 12. Microglia induced to take up iron show changes in molecular expression suggestive of changes in ER stress and autophagy. The consequence of these changes is the adoption of a senescence associates secretory phenotype and changes in the release of a variety of proteins including cytokines and enzymes like IDE. Decreased release of IDE results in decreased breakdown of β-amyloid released by neuronal cells. These findings provide a potential mechanistic insight into how microglial aging can contribute to the accumulation of β-amyloid and advance the pathology of AD.

METHODS

Unless otherwise stated reagents were purchased from Sigma-Aldrich.

Cell Culture

The microglia cell line used in this study was the SV40 immortalised human microglia cell line (ABM). Cells were cultured in DMEM with 4.5 g/L glucose (LONZA) supplemented with 10% FBS (Labtec), and 1% pen/strep. Cells were maintained at 37^{o}C and 5% CO_2 in a humidified incubator. The neuronal cell line used in experiments was the SH-SY5Y human neuroblastoma. This cell line was grown under the same conditions as the microglial cell line. Images of microglia were either produced using a Nikon Diaphot-TMD inverted microscope (live cells) or Nikon Eclipse E800 microscope (stained cells). Perl's staining was performed using a kit from Atom Scientific. Control and iron-fed microglial cells were plated onto cover slips and left overnight. They were washed in PBS and fixed in ice-cold methanol for 5 min at -20^{o}C. The cells were stained according to the manufacturer's instructions and mounted onto slides using glycerol jelly as mounting medium.

Microglia were cultured in high iron conditions to induce a senescent phenotype. The iron stock solution used was 25mM ferric ammonium citrate(Acros Organics) prepared in deionised water and filtered through a 0.22μm syringe filter (Millipore) Microglial cell lines were grown in medium containing in 500 μM ferric ammonium citrate for a minimum of two weeks. Cell lines were maintained under these conditions until used for experiments. Conditioned medium was produced from the microglia by washing them with serum free medium (DMEM) to remove excess iron and then growing them for 48 h in DMEM supplement with B27 without antioxidants (Gibco) plus 1% Penicillin and Streptomycin. The conditioned medium was collected

from both control and iron-fed microglia and centrifuged to remove debris and filtered through a 0.45 μm filter before use in further experiments.

Drug treatments were for 16 h or 24 h. Brefeldin A (10mM), Bafilomycin (2μM) and tunicamycin (1.2mM) were prepared as stock solutions in methanol. Concentrated stocks of the IDE inhibitor ML345 (10.4mM) and the neprilysin inhibitor thiorphan (1mM) were prepared as concentrated stocks in DMSO. Synthetic β-amyloid was from Meso Scale Discovery.

Western Blot

Cells were lysed in PBS with 0.5% Igepal CA-630 and 'complete' protease inhibitor cocktail (Roche), sonicated 5 seconds on ice, incubated on ice for 20 min and centrifuged 10 000 x g for 5 min to remove insoluble membranes. Protein concentration was determined with a Bradford protein assay (Bio-Rad), according to the manufacturer's instructions. Protein concentrations were normalized and samples were boiled for 5 min with 1 x Laemmli SDS-PAGE buffer. Samples were loaded into either a 10% or a 14% (depending on molecular weight of the protein) acrylamide SDS-PAGE gel, with a buffer of Tris (250 mM) + Glycine (1.92 M) + SDS (0.1% w/v), run at 250V and 35mA/gel for 45-60 min. Separated proteins were transferred to a PVDF membrane (Millipore) by a semi-dry transfer apparatus, run at 25V and 100mA/gel for 1.5 h. Membranes were blocked in 5% w/v non-fat milk powder in Tris buffered saline + 0.1% Tween 20 (TBS-T) for one hour, incubated with primary antibody for 1-2 h or overnight, and washed 3 x 15 min in TBS-T. Membranes were blocked again for 10 min and incubated with horseradish peroxidase-conjugated secondary antibody (DAKO) for one hour. A further 3 x 15

min washes were performed, and the membranes developed with Luminata Crescendo or Luminata Forte ECL substrate (Thermo Scientific), and imaged with a Fusion SL CCD imaging system (Vilber Lourmat). Antibodies used in this study included, rabbit anti-ferritin light chain (ab69090, Abcam), rabbit anti-KV1.3 (APC101, Alomone Labs), mouse anti-GAPDH (ab8245, Abcam), mouse anti-alpha-tubulin (B512, Sigma), anti-APP (ab133509, Abcam), rabbit anti-ADAM10 (Millipore), rabbit anti-BACE1 (Cell Signalling Technology) mouse anti-SIRT1 (1F3, Cell Signaling Technology), rabbit anti-insulin degrading enzyme (EPR6099, Abcam), rabbit anti-LC3 (ab48394, Abcam), rabbit anti-MTOR (PA1-518, ThermoFisher), rabbit anti-phospho-MTOR (S2448, ab109268, Abcam), rabbit anti-EIF2a (Cell Signalling Technology), rabbit anti-phospho-eIF2a (Ser51, Cell Signalling Technology, rabbit anti- NF-κB p65 (D14E12, Cell Signalling Technology), rabbit anti-acetyl-NF-κB p65, (Lys310, Cell Signalling Technology), rabbit anti-FMRP (ab17722, Abcam) and rabbit anti-SCAMP5 (ab3432, Abcam). Densitometric analysis was performed on Image J.

Iron Assay

The levels of total iron in human microglia were determined using a commercial assay (Abcam) and following the manufacturer's instructions. Cellular iron content was determined from four confluent T25 flasks and normalized to total protein content determined by the Bradford assay.

Glutamate Assay

Glutamate levels in conditioned medium were assessed using a commercial kit according to the manufacturer's instructions (Sigma). Microglia were plated out at

equivalent densities and conditioned medium was generated as described above. After collection of the conditioned medium the microglia were lysed and protein concentration was measured using the Bradford assay. The glutamate concentrations were normalised to protein content in the lysates.

ADAM10 Activity Assay

The enzymatic activity of ADAM10 in SH-SY5Y cells was assessed using a commercial kit according to the manufacturer's instructions (Anaspec). Confluent SH-SY5Y cells were treated with SFM or conditioned medium from microglia for 24h. The cells were lysed and protein concentrations were measured using the Bradford assay. Equivalent amounts of protein were used in the ADAM10 activity assay to account for differences in cell number. Readings were taken at 520nm every 5 min and the initial rate was calculated for each condition.

Promoter Assay

The ADAM10 promoter construct was a gift and was as previously described [102]. SH-SY5Y cells were grown in 24-well plates seeded at 5×10^4 cells/well 24 h prior to transfection. Transfections of the promoter construct in pGL Basic (with firefly luciferase activity) were performed using FuGENE HD® transfection reagent (Promega) as per manufacturer's instructions. To control for variation in transfection efficiency among replicates, promoter constructs were co-transfected with the Renilla luciferase vector, pRL-TK (Promega). At 24h post transfection, SH-SY5Y cells were harvested and firefly and Renilla luciferase chemiluminescence were measured using the Dual-Luciferase® Reporter Assay System (Promega) in a BMG FLUOstar

Omega plate reader (BMG Labtech GmbH). Luciferase activity was calculated as the ratio of firefly to Renilla luciferase activity.

APP cleavage Luciferase reporter Assay

The luciferase reporter assays was carried out as previously described [103]. SH-SY5Y cells were plated out at 5 × 10^4 cells/well in 24 well plates in triplicate for each condition and left to re-attach for 18-24 h at 37^{o}C, 5% CO2. Test wells were transfected with plasmids pFR-Luc (A firefly luciferase reporter construct pFR controlled by a synthetic promoter made of five tandem repeats of the yeast GAL4 activation sequence followed by a minimal TATA box), APP-Gal4 (pRC-CMV vector containing APP695 cDNA and a Gal4-DNA binding domain fused to its C-terminal. Cleavage of the AICD domain with Gal-4 domain attached leads to it binding to the pFR vector and expressing firefly luciferase) and pRL-TK (containing *Renilla* luciferase as above) using the transfection reagent Fugene HD. Control wells were transfected with pFR-Luc and pRL-TK only to assess background luciferase activity. The cells were transfected for approximately 24 h and then treated with SFM or microglial conditioned medium for 24 h. After lysing and harvesting the cells firefly luciferase and *Renilla* luciferase activity were measured with the Dual-Luciferase® Reporter Assay System on a FLUOstar Omega plate reader. Luciferase activity was calculated as the ratio of firefly to *Renilla* luciferase activity.

Proliferation Assay

Proliferation of C8B4 microglia was assessed using the Abcam BrdU proliferation ELISA kit (Abcam, ab126556) according the manufacturer's instructions. Both untreated and iron-fed human microglia were plated at equal density ranging from

2000 to 20,000 cells per well in 96 well trays. The cells were exposed to BrdU (bromodeoxyuridine) for 24 h prior to starting the assay. Absorbance was measured at 450 nm in a FLUOstar Omega plate reader following the colorimetric assay.

β-Amyloid Assay

Concentrations of β-Amyloid (both 1-40 and 1-42) present in cell culture medium were determined using the Meso Scale Discovery (MSD) Sector Imager S 600 multiplex plate reader. The plate used for the analysis was the V-Plex Aβ Peptide Panel kit 1 (MSD). Medium was collected from SH-SY5Y cells that had been exposed either to conditioned medium or control medium (DMEM with B27 supplement) as described above and filtered through a 0.22 μm filter before applying to the plate without dilution. Concentrations were determined by comparison to a standard curve for each individual β-Amyloid peptide. The values were adjusted for plating density by assessing the protein content of the cells used to generate the conditioned medium using the Bradford assay and dividing the β-Amyloid concentration by the protein concentration.

Cytokine Assay.

Cytokines secreted by the human microglia were also measured using the MSD Sector Imager S 600 multiplex plate reader. The cytokines were assessed using the V-PLEX Proinflammatory Panel 1 Human Kit (MSD). This kit measured IFN-γ, IL-10, IL-12p70, IL-13, IL-1β, IL-2, IL-4, IL-6, IL-8 and TNF-α. Conditioned medium was collected from control and iron-fed microglia as described above. The microglia used to generate the conditioned medium were lysed and their protein content was measured using a Bradford Assay to account for differences in cell number.

Statistics

All statistics were carried out in Microsoft Excel. Statistical analyses were conducted using a two-tailed Student's t test, statistical significance at *p*-value of < 0.05. Data are expressed as the mean ± standard error (S.E.).

SUPPORTING INFORMATION: (A figure showing the effect of Iron on β-amyloid in SH-SY5Y cell medium)

AUTHOR CONTRIBUTION

DRB obtained the funding and devised the project. All other aspects of the work were performed by DMA and DRB.

CONFLICT OF INTEREST

The authors declare no conflict of interest

FUNDING SOURCE

The research was supported by a PhD Studentship from the Bristol charity BRACE.

ACKNOWLEDGEMENTS

The authors thank Falk Fahrenholz for the ADAM10 promoter reporter.

Cytokine (ng/mg)	**Control**	**Iron-fed**
IL-8	47211.41 ± 19621.34	120271.14 ± 22992.87*
IL-6	3393.33 ± 1501.62	14181.68 ± 2346.10*
IL-1b	35.95 ± 12.72	115.31 ± 23.87*
IL-13	1.05 ± 0.16	1.47 ± 0.29
IL-10	0.03 ± 0.00	0.05 ± 0.01
IL-2	0.05 ± 0.04	0.15 ± 0.02
TNFα	0.88 ± 0.47	0.16 ± 0.08
IFNγ	ND	ND
IL-4	ND	ND
IL-12p70	ND	ND

Table 1 Cytokine released into conditioned medium
Serum free conditioned medium was generated from cultured microglia over 24 h and the levels of cytokines assessed with the MSD ELISA system. Cytokine concentrations were determined by comparison to a standard curve for each cytokine. Values were the concentration in the medium (ng/mL) divided by the concentration of the protein in the cells that were used to generate the conditioned medium (mg/mL). Shown are the mean (ng/mg) and s.e. for four experiments. * Indicates a significant difference between control and iron-fed (p-value <0.05). n.d. indicates not detectible due to the levels detected being below the level of lowest standard on the standard curve for that cytokine.

Protein (Relative value, Units)	**Control**	**Iron-fed**
Total mTOR	1.6 ± 0.2	1.8 ± 0.2
Ratio p-mTor/T-mtor	1.0 ± 0.1	4.2 ± 0.7 *
Total eIF2a	1.1 ± 0.2	1.0 ± 0.1
Ratio p-eIF2a /T-eIF2a	1.0 ± 0.3	2.3 ± 0.3 *
FMRP	1.0 ± 0.2	2.3 ± 0.3 *
SCAMP-5	1.0 ± 0.2	2.4 ± 0.4 *
Total NF-κB	1.1 ± 0.2	1.0 ± 0.2
Ratio Acetyl-NF-κB/T-NF-κB	1.0 ± 0.3	2.6 ± 0.7 *

Table 2 Altered Expression of Protein in Iron-Fed microglia
Densitometric analysis of the bands on western blots shown in Figure 10. Total levels of mTOR, eIF2a and NF-κB were assessed as well as the ratio of the modified (p or acetyl) form to the total form (T). Shown are mean and s.e. for 4-8 experiments each.* Indicates a significant difference between control and iron-fed ($p < 0.05$).

FIGURE LEGENDS

Figure 1 iron-fed microglia in culture

Photomicrographs of human immortalized microglia in culture **A** Microglia grown in control conditions showed many fine process (arrows) **B** Microglia grown in 500 μM ferric ammonium citrate (iron-fed) for at least two weeks showed a loss of these processes. Arrows indicated more amoeboid appearance. Scale bar = 100 μm.

Figure 2 Iron and ferritin in iron-fed microglia

Perl's Stain is a traditional stain for the detection of iron deposits in cells. Cultured microglia were stained using Perl's stain. Iron deposits appear blue following the procedure. **A** Control microglia show no obvious staining while **B** Iron-fed microglia (grown in iron for at least two weeks) show extensive blue staining in almost all cells (arrows). **C** Western blotting was used to detect ferritin in protein extracts from control and iron-fed microglia. GAPDH was used as loading control. **D** Densitometric analysis of ferritin expression was normalized to GAPDH levels (relative value). Iron-fed microglia show significantly higher levels of ferritin expression ($p < 0.05$) when compared to controls. Shown are the mean and s.e. of four experiments. **E** The level of iron was detected in extracts from microglia using a commercial kit. The iron-fed microglia showed very high and significantly different ($p < 0.05$) levels of iron when compared to controls. Shown are the mean and s.e. of four experiments.

Figure 3 Proliferation of iron-fed microglia

The rate of proliferation of human immortalized microglia was assessed using a BrdU based ELISA kit. Both control and iron-fed microglia were plated into a 96 well plate at a range of densities and grown overnight. BrdU was then added for a further

16 h before the ELISA assay was used to assess incorporation levels. The level of incorporation was assessed by a colorimetric assay with a read out at 450 nm. Iron-fed microglia showed no significant difference in proliferation at all plating densities ($p > 0.05$). Shown are the mean and s.e. of four separate experiments.

Figure 4 Glutamate release and protein expression iron-fed microglia

A The release of glutamate by human immortalized microglia was assessed with a commercial glutamate assay kit. Control and iron-fed microglia plated at equal density were grown in serum free medium for 48 h. The level of glutamate was then determined after collecting the medium. The protein content of the conditioning cells was determined in parallel. Glutamate concentration was assessed relative to the protein content of the cells to account for differences in cell number. Iron-fed microglia released significantly less glutamate than control microglia ($p < 0.05$). **B** Western blotting was used to assess the level of expression of KV1.3 in protein extracts from control and iron-fed microglia. A specific antibody was used to detect KV1.3 and GAPDH. **C** Western blotting was used to assess the level of expression of SIRT-1 in protein extracts from control and iron-fed microglia. A specific antibody was used to detect SIRT-1 and GAPDH. **D** Densitometric analysis of KV1.3 and SIRT-1. Expression was normalized to GAPDH levels (relative value). Iron-fed microglia show significantly higher levels of KV1.3 expression ($p < 0.05$) and significantly lower SIRT-1 expression ($p < 0.05$) when compared to controls.

* indicates significant difference. Shown are the mean and s.e. of four experiments for all parts.

Figure 5 Effects of microglial conditioned medium on protein expression.

Conditioned medium was prepared from control and iron-fed microglia. The conditioned medium was applied to SH-SY5Y cells for 24 h. Extracts were prepared from the SH-SY5Y cells along with cells that had been treated only with serum free medium (SFM). The extracts were applied to a PAGE gel, and the gel western blotted. APP, ADAM10, BACE-1 and tubulin (loading control) were detected on the resultant membrane with specific antibodies. Following detection, the intensity of the bands was assessed using densitometry. **A-B.** Analysis of APP expression in SH-SY5Ys showed there was no significant ($p > 0.05$) effect of either control or iron-fed conditioned medium. The same result was seen whether the individual bands were quantitated together or separately.

C-D. In contrast, treatment of SH-SY5Y cells with conditioned medium from iron-fed microglia (but not control) reduced the protein expression of ADAM10 significantly ($p < 0.05$) when compared to SFM. **E-F.** There was no significant effect of either microglial conditioned medium on the expression of BACE-1 in SH-SY5Y cells. Shown are the mean and s.e. for four experiments each. * indicates a significant difference when compared to SFM.

Figure 6 Investigation of microglia induced changes in ADAM10

A The level of APP cleavage in SH-SY5Y cells was measured using a dual luciferase reporter assay. The assay is based upon binding of a GAL-4 DNA binding domain to the DNA sequence in the luciferase reporter construct. Binding is directly proportional to the release of the ACID domain from APP to which the GAL-4 domain is fused. SH-SY5Y cells transfected with the reporter constructs were treated for 24

h with conditioned medium from control and iron-fed microglia or with serum free medium (SFM). Activity measured from the firefly luciferase reporter construct reporting AICD release was divided by *Renilla* luciferase control activity (pTK) to give relative luciferase activity for each treatment. Conditioned medium from both control and iron-fed microglia caused a significant reduction in the luciferase activity measured ($p < 0.05$) compared to SFM. However, there was no significant difference when comparing the effect of control and iron-fed microglia conditioned medium to each other.

B The level of ADAM10 promoter activity was assessed in SH-SY5Y cells. The cells were transiently transfected with the luciferase reporter construct carrying the ADAM10 promoter and the control reporter (pTK). The cells were treated with conditioned medium from control and iron-fed microglia for 24 h. The level of luciferase activity was then assessed and compared to that measured in the SFM control. Neither control nor iron-fed microglial conditioned medium had a significant ($p >0.05$) effect on luciferase activity.

C The level of ADAM10 activity in SH-SY5Y cells was assessed with a commercial kit. The kit measured fluorescent activity following cleavage of an ADAM10 substrate by ADAM10 present in extracts from the cells. Extracts were prepared from SH-SY5Y cells treated for 24 h with conditioned medium from control or iron-fed microglia or SFM. Fluorescence was measured at 520 nm in a plate reader following application of extract to the assay. The values were adjusted to the protein concentration of the extracts. Treatment of SH-SY5Y cells with microglia conditioned medium had no significant effect ($p > 0.05$) on measured ADAM10 activity.

D-E FMRP is translation inhibitor known to influence protein expression of ADAM10. We measured FMRP expression in protein extracts from SH-SY5Y cells by western

blot. SH-SY5Y cells were treated with conditioned medium from control and iron-fed microglia or SFM. After 24 h protein extracts were prepared from the SH-SY5Y cells and applied to the western blot procedure. FMRP and tubulin (loading control) were detected with specific antibodies and the band intensity after chemiluminescence detection assessed with densitometry. Conditioned medium from iron-fed microglia but not control microglia had significant effect on FMRP detected in SH-SY5Y cells ($p < 0.05$), greatly increasing the level detected.

Shown are the mean and s.e. for four experiments in all cases. * indicates a significant difference when compared to SFM.

Figure 7 Microglia degradation of β-amyloid

We used an MSD Sector Imager to measure the levels of β-amyloid in culture medium. The multiplex MSD assay measured both $A\beta_{1-40}$ and $A\beta_{1-42}$ simultaneously in the same experiments.

A-B SH-SY5Y cells were treated with conditioned medium from control and iron-fed microglia. The levels of β-amyloid released after 24 h were assessed and compared to that of SH-SY5Y cells grown in serum free medium alone (SFM). The levels of both $A\beta_{1-40}$ and $A\beta_{1-42}$ were significantly ($p < 0.05$) reduced after either treatment. However, the levels of both peptides were significantly higher when SH-SY5Y cells were treated with medium from iron-fed microglia than they were when treated with medium from control microglia.

C-D Synthetic $A\beta_{1-40}$ and $A\beta_{1-42}$ were treated with conditioned medium from control and iron-fed microglia or SFM for 24 h. The conditioned medium was diluted with SFM. After this time the levels of β-amyloid remaining were assessed with the MSD assay. In the SFM controls 904 ± 141 ng/mL $A\beta_{1-40}$ and 157 ± 27 ng/mL $A\beta_{1-42}$ were

detected. The amount remaining in the conditioned medium treated wells is shown as a percentage of these values. At both 50% and 25% conditioned medium there was significantly more $A\beta_{1-40}$ and $A\beta_{1-42}$ remaining under iron-fed conditions than control ($p < 0.05$) implying that conditioned medium from iron-fed microglia degraded both forms of β-amyloid less than control microglial conditioned medium.

E-F The experiment with synthetic $A\beta_{1-40}$ and $A\beta_{1-42}$ was repeated but with the addition of enzyme inhibitors. $A\beta_{1-40}$ and $A\beta_{1-42}$ were treated with conditioned medium from control and iron-fed microglia with the addition for either DMSO vehicle, IDE inhibitor or neprylisin (NEP) inhibitor. After 24 h the levels of $A\beta_{1-40}$ and $A\beta_{1-42}$ remaining were assessed with the MSD assay. In the SFM controls 3715 ± 385 ng/mL $A\beta_{1-40}$ and 246 ± 42 ng/mL $A\beta_{1-42}$ were detected. Compared to the DMSO control, the NEP inhibitor had no significant effect on the levels detected for either control or iron-fed conditioned while the IDE inhibitor significantly reduced degradation of both $A\beta_{1-40}$ and $A\beta_{1-42}$ ($p < 0.05$).

G-H The levels of IDE were measured in both control and iron fed microglia and also in the conditioned medium generated from these cells. The relative levels of IDE were measured using western blotting and detection with a specific antibody. GAPDH was measured as a control for loading of the cell lysates. The conditioned media from the microglia were concentrated 10-fold with a 30kDa centrifugal filter (Sartorius) to increase chances of detection. After western blotting the detected bands were densitometrically quantitated. The levels of IDE in the cells were not significantly different between control and iron-fed microglia while that released into the medium was significantly ($p < 0.05$) reduced for iron-fed microglia.

For all sections shown are the mean and s.e. for at least four independent experiments. * indicates a significant different between treatment and control. †

indicated a significant difference between treatments with conditioned medium from control and iron-fed microglia.

Figure 8 Autophagy in iron-fed microglia

The levels of LC3-II were determined in human microglia by western blot. Control and iron-fed microglia were grown in serum free medium (SFM) and treated either with 13 nM bafilomycin (Bafilo) or the equivalent volume of methanol (20 μL, 0.67% of total volume). After 16 h protein extracts were prepared from the cells and applied to a 14% PAGE gel. After transfer to a membrane the presence of LC3-II and GAPDH (loading control) were detected with specific antibodies. After chemiluminescent detection to visualize the bands (upper panel) the intensity of the bands was assessed with densitometry. Iron-fed cells grown in SFM showed significantly higher levels of LC3-II than control microglia ($p < 0.05$). Treatment with bafilomycin significantly increased the levels of LC3-II for control microglia but not for iron-fed microglia. Shown are the mean and s.e. for seven experiments. * indicates a significant difference between treatment and methanol control. † indicated a significant difference between control and iron-fed microglia.

Figure 9 Expression of proteins related to autophagy and ER stress

Protein extracts were prepared from control and iron-fed microglia. Western blotting and immunodetection were used to assess the level of expression of a range of proteins. These proteins were **A** phosphorylated-MTOR (p-MTOR) and total MTOR (T-MTOR), **B** phosphorylated-EIF2a (p- EIF2a) and total EIF2a (T- EIF2a), **C** FMRP, **D** SCAMP5 and **E** acetyl-NF-κB and total NF-κB (T-NF-κB). In each case GAPDH

was also analysed to ensure equal loading of the samples. Quantitation appears in Table 2.

Figure 10 Autophagy, ER stress and IDE release

The levels of IDE were measured in cell extracts from control microglia with and without treatment with either with 13 nM bafilomycin, 0.1 μg/mL brefeldin A, or 1.0 μg/mL tunicamycin. The treatments were for 16 h and after that time conditioned medium generated from these cells was collected and protein extracts made from the cells. The relative levels of IDE were measured using western blot and detection with a specific antibody GAPDH was measured as a control for loading of the cell lysates. The conditioned media from the microglia were concentrated 10 fold to increase chances of detection. After western blot the detected bands were densitometrically quantitated. None of the treatments increased IDE levels in the microglia but all treatments caused a significant decrease ($p < 0.05$) in IDE detected in the medium when compared to the control. Shown are the mean and s.e. from seven independent experiments.

Figure 11 Autophagy, ER stress and β-amyloid

Synthetic $A\beta_{1\text{-}40}$ and $A\beta_{1\text{-}42}$ were treated with conditioned medium from control microglia treated either with 13 nM bafilomycin, 100 ng/mL brefeldin A, 1.0 μg/mL tunicamycin or SFM alone for 16 h. After this time the levels of β-amyloid remaining were assessed with the MSD assay. In the SFM controls 3326 ± 240 ng/mL $A\beta_{1\text{-}40}$ and 231 ± 10 ng/mL $A\beta_{1\text{-}42}$ were detected. All three treatments significantly increased ($p < 0.05$) the level of $A\beta_{1\text{-}40}$ and $A\beta_{1\text{-}42}$ detected when compared to control microglia conditioned medium. Shown are the mean and s.e. for four experiments.

Figure 12 Model of Dystrophic Microglial induced increase in β-amyloid

A summary figure illustrating the changes we have observed in this study. Excess uptake of iron by microglia induces a dystrophic-like phenotype illustrated by changes in Ferritin expression and iron storage. Increased cellular iron also increases the labile iron pool with the consequence of increased oxidative events which are known to induce ER stress. The consequence of induced ER stress is changes in markers such as SCAMP5 and EIF2a and altering protein translation through FMRP. One consequence of induced action of FMRP is the decreased expression of the deacetylase SIRT-1 resulting in higher levels of acetylated-NF-κB. This change is known to result in increased release of pro-inflammatory cytokines indicating a switch in the secretory phenotype to one associated with cell senescence. Decreased SIRT1 activity is also associated with increased phosphorylation of MTOR, resulting in reduced autophagy. Decreased autophagy causes an increase in the levels of LC3-II by reduction in its turnover. It also results in a decrease in the secretion of proteins that include IDE. Reduced IDE then results in increased extracellular levels of β-amyloid.

REFERENCES

[1] Wyss-Coray, T. (2016) Ageing, neurodegeneration and brain rejuvenation, *Nature 539*, 180-186.
[2] Jorm, A. F. (1997) Alzheimer's disease: risk and protection, *Med J Aust 167*, 443-446.
[3] Mastrianni, J. A. (2010) The genetics of prion diseases, *Genet Med 12*, 187-195.
[4] Bateman, R. J., Aisen, P. S., De Strooper, B., Fox, N. C., Lemere, C. A., Ringman, J. M., Salloway, S., Sperling, R. A., Windisch, M., and Xiong, C. (2011) Autosomal-dominant Alzheimer's disease: a review and proposal for the prevention of Alzheimer's disease, *Alzheimers Res Ther 3*, 1.
[5] Mitchell, S. J., Scheibye-Knudsen, M., Longo, D. L., and de Cabo, R. (2015) Animal models of aging research: implications for human aging and age-related diseases, *Annu Rev Anim Biosci 3*, 283-303.
[6] Campos, P. B., Paulsen, B. S., and Rehen, S. K. (2014) Accelerating neuronal aging in in vitro model brain disorders: a focus on reactive oxygen species, *Front Aging Neurosci 6*, 292.
[7] de Magalhaes, J. P. (2004) From cells to ageing: a review of models and mechanisms of cellular senescence and their impact on human ageing, *Exp Cell Res 300*, 1-10.
[8] Whalley, K. (2017) Microglia: A protective population?, *Nature reviews. Neuroscience 18*, 454.
[9] Leyns, C. E. G., and Holtzman, D. M. (2017) Glial contributions to neurodegeneration in tauopathies, *Molecular neurodegeneration 12*, 50.
[10] Colonna, M., and Butovsky, O. (2017) Microglia Function in the Central Nervous System During Health and Neurodegeneration, *Annual review of immunology 35*, 441-468.
[11] Blaylock, R. L. (2017) Parkinson's disease: Microglial/macrophage-induced immunoexcitotoxicity as a central mechanism of neurodegeneration, *Surg Neurol Int 8*, 65.
[12] von Bernhardi, R., Eugenin-von Bernhardi, L., and Eugenin, J. (2015) Microglial cell dysregulation in brain aging and neurodegeneration, *Frontiers in aging neuroscience 7*, 124.
[13] Siskova, Z., and Tremblay, M. E. (2013) Microglia and synapse: interactions in health and neurodegeneration, *Neural plasticity 2013*, 425845.
[14] Lassmann, H., and van Horssen, J. (2011) The molecular basis of neurodegeneration in multiple sclerosis, *FEBS letters 585*, 3715-3723.
[15] Perry, V. H. (2010) Contribution of systemic inflammation to chronic neurodegeneration, *Acta neuropathologica 120*, 277-286.
[16] Boche, D., Perry, V. H., and Nicoll, J. A. (2013) Review: activation patterns of microglia and their identification in the human brain, *Neuropathology and applied neurobiology 39*, 3-18.
[17] Streit, W. J., Sammons, N. W., Kuhns, A. J., and Sparks, D. L. (2004) Dystrophic microglia in the aging human brain, *Glia 45*, 208-212.
[18] Streit, W. J., Xue, Q. S., Tischer, J., and Bechmann, I. (2014) Microglial pathology, *Acta neuropathologica communications 2*, 142.
[19] Chinta, S. J., Woods, G., Rane, A., Demaria, M., Campisi, J., and Andersen, J. K. (2015) Cellular senescence and the aging brain, *Experimental gerontology 68*, 3-7.
[20] Flanary, B. (2005) The role of microglial cellular senescence in the aging and Alzheimer diseased brain, *Rejuvenation research 8*, 82-85.

[21] Simmons, D. A., Casale, M., Alcon, B., Pham, N., Narayan, N., and Lynch, G. (2007) Ferritin accumulation in dystrophic microglia is an early event in the development of Huntington's disease, *Glia 55*, 1074-1084.

[22] Lopes, K. O., Sparks, D. L., and Streit, W. J. (2008) Microglial dystrophy in the aged and Alzheimer's disease brain is associated with ferritin immunoreactivity, *Glia 56*, 1048-1060.

[23] Bartzokis, G., Tishler, T. A., Shin, I. S., Lu, P. H., and Cummings, J. L. (2004) Brain ferritin iron as a risk factor for age at onset in neurodegenerative diseases, *Annals of the New York Academy of Sciences 1012*, 224-236.

[24] Gregory, A., and Hayflick, S. (1993) Neurodegeneration with Brain Iron Accumulation Disorders Overview, In *GeneReviews(R)* (Adam, M. P., Ardinger, H. H., Pagon, R. A., Wallace, S. E., Bean, L. J. H., Mefford, H. C., Stephens, K., Amemiya, A., and Ledbetter, N., Eds.), Seattle (WA).

[25] Ward, R. J., Zucca, F. A., Duyn, J. H., Crichton, R. R., and Zecca, L. (2014) The role of iron in brain ageing and neurodegenerative disorders, *Lancet Neurol 13*, 1045-1060.

[26] Dexter, D. T., Wells, F. R., Agid, F., Agid, Y., Lees, A. J., Jenner, P., and Marsden, C. D. (1987) Increased nigral iron content in postmortem parkinsonian brain, *Lancet 2*, 1219-1220.

[27] Belaidi, A. A., and Bush, A. I. (2016) Iron neurochemistry in Alzheimer's disease and Parkinson's disease: targets for therapeutics, *J Neurochem 139 Suppl 1*, 179-197.

[28] Streit, W. J., Braak, H., Xue, Q. S., and Bechmann, I. (2009) Dystrophic (senescent) rather than activated microglial cells are associated with tau pathology and likely precede neurodegeneration in Alzheimer's disease, *Acta neuropathologica 118*, 475-485.

[29] Haass, C., and Selkoe, D. J. (1993) Cellular processing of beta-amyloid precursor protein and the genesis of amyloid beta-peptide, *Cell 75*, 1039-1042.

[30] Ittner, L. M., and Gotz, J. (2011) Amyloid-beta and tau--a toxic pas de deux in Alzheimer's disease, *Nat Rev Neurosci 12*, 65-72.

[31] Lee, C. Y., and Landreth, G. E. (2010) The role of microglia in amyloid clearance from the AD brain, *J Neural Transm (Vienna) 117*, 949-960.

[32] Zuroff, L., Daley, D., Black, K. L., and Koronyo-Hamaoui, M. (2017) Clearance of cerebral Abeta in Alzheimer's disease: reassessing the role of microglia and monocytes, *Cell Mol Life Sci 74*, 2167-2201.

[33] Zotova, E., Holmes, C., Johnston, D., Neal, J. W., Nicoll, J. A., and Boche, D. (2011) Microglial alterations in human Alzheimer's disease following Abeta42 immunization, *Neuropathology and applied neurobiology 37*, 513-524.

[34] Meda, L., Baron, P., and Scarlato, G. (2001) Glial activation in Alzheimer's disease: the role of Abeta and its associated proteins, *Neurobiology of aging 22*, 885-893.

[35] Koellhoffer, E. C., McCullough, L. D., and Ritzel, R. M. (2017) Old Maids: Aging and Its Impact on Microglia Function, *International journal of molecular sciences 18*.

[36] Caldeira, C., Oliveira, A. F., Cunha, C., Vaz, A. R., Falcao, A. S., Fernandes, A., and Brites, D. (2014) Microglia change from a reactive to an age-like phenotype with the time in culture, *Frontiers in cellular neuroscience 8*, 152.

[37] Schilling, T., and Eder, C. (2015) Microglial K(+) channel expression in young adult and aged mice, *Glia 63*, 664-672.

[38] Charolidi, N., Schilling, T., and Eder, C. (2015) Microglial Kv1.3 Channels and P2Y12 Receptors Differentially Regulate Cytokine and Chemokine Release from Brain Slices of Young Adult and Aged Mice, *PloS one 10*, e0128463.

[39] Cho, S. H., Chen, J. A., Sayed, F., Ward, M. E., Gao, F., Nguyen, T. A., Krabbe, G., Sohn, P. D., Lo, I., Minami, S., Devidze, N., Zhou, Y., Coppola, G., and Gan, L.

(2015) SIRT1 deficiency in microglia contributes to cognitive decline in aging and neurodegeneration via epigenetic regulation of IL-1beta, *The Journal of neuroscience : the official journal of the Society for Neuroscience 35*, 807-818.

[40] Roberts, H. L., Schneider, B. L., and Brown, D. R. (2017) alpha-Synuclein increases beta-amyloid secretion by promoting beta-/gamma-secretase processing of APP, *PLoS One 12*, e0171925.

[41] Lammich, S., Kamp, F., Wagner, J., Nuscher, B., Zilow, S., Ludwig, A. K., Willem, M., and Haass, C. (2011) Translational repression of the disintegrin and metalloprotease ADAM10 by a stable G-quadruplex secondary structure in its 5'-untranslated region, *J Biol Chem 286*, 45063-45072.

[42] Qiu, W. Q., Walsh, D. M., Ye, Z., Vekrellis, K., Zhang, J., Podlisny, M. B., Rosner, M. R., Safavi, A., Hersh, L. B., and Selkoe, D. J. (1998) Insulin-degrading enzyme regulates extracellular levels of amyloid beta-protein by degradation, *The Journal of biological chemistry 273*, 32730-32738.

[43] Hickman, S. E., Allison, E. K., and El Khoury, J. (2008) Microglial dysfunction and defective beta-amyloid clearance pathways in aging Alzheimer's disease mice, *The Journal of neuroscience : the official journal of the Society for Neuroscience 28*, 8354-8360.

[44] Abdul-Hay, S. O., Bannister, T. D., Wang, H., Cameron, M. D., Caulfield, T. R., Masson, A., Bertrand, J., Howard, E. A., McGuire, M. P., Crisafulli, U., Rosenberry, T. R., Topper, C. L., Thompson, C. R., Schurer, S. C., Madoux, F., Hodder, P., and Leissring, M. A. (2015) Selective Targeting of Extracellular Insulin-Degrading Enzyme by Quasi-Irreversible Thiol-Modifying Inhibitors, *ACS Chem Biol 10*, 2716-2724.

[45] Shirotani, K., Tsubuki, S., Iwata, N., Takaki, Y., Harigaya, W., Maruyama, K., Kiryu-Seo, S., Kiyama, H., Iwata, H., Tomita, T., Iwatsubo, T., and Saido, T. C. (2001) Neprilysin degrades both amyloid beta peptides 1-40 and 1-42 most rapidly and efficiently among thiorphan- and phosphoramidon-sensitive endopeptidases, *J Biol Chem 276*, 21895-21901.

[46] Son, S. M., Cha, M. Y., Choi, H., Kang, S., Choi, H., Lee, M. S., Park, S. A., and Mook-Jung, I. (2016) Insulin-degrading enzyme secretion from astrocytes is mediated by an autophagy-based unconventional secretory pathway in Alzheimer disease, *Autophagy 12*, 784-800.

[47] Gomez-Sanchez, R., Pizarro-Estrella, E., Yakhine-Diop, S. M., Rodriguez-Arribas, M., Bravo-San Pedro, J. M., Fuentes, J. M., and Gonzalez-Polo, R. A. (2015) Routine Western blot to check autophagic flux: cautions and recommendations, *Analytical biochemistry 477*, 13-20.

[48] Xie, Z., Xie, Y., Xu, Y., Zhou, H., Xu, W., and Dong, Q. (2014) Bafilomycin A1 inhibits autophagy and induces apoptosis in MG63 osteosarcoma cells, *Molecular medicine reports 10*, 1103-1107.

[49] Oliveira, S. J., de Sousa, M., and Pinto, J. P. (2011) ER Stress and Iron Homeostasis: A New Frontier for the UPR, *Biochem Res Int 2011*, 896474.

[50] Perluigi, M., Di Domenico, F., and Butterfield, D. A. (2015) mTOR signaling in aging and neurodegeneration: At the crossroad between metabolism dysfunction and impairment of autophagy, *Neurobiology of disease 84*, 39-49.

[51] Rashid, H. O., Yadav, R. K., Kim, H. R., and Chae, H. J. (2015) ER stress: Autophagy induction, inhibition and selection, *Autophagy 11*, 1956-1977.

[52] Noh, J. Y., Lee, H., Song, S., Kim, N. S., Im, W., Kim, M., Seo, H., Chung, C. W., Chang, J. W., Ferrante, R. J., Yoo, Y. J., Ryu, H., and Jung, Y. K. (2009) SCAMP5 links endoplasmic reticulum stress to the accumulation of expanded polyglutamine

protein aggregates via endocytosis inhibition, *The Journal of biological chemistry 284*, 11318-11325.

[53] Yu, Z., Fan, D., Gui, B., Shi, L., Xuan, C., Shan, L., Wang, Q., Shang, Y., and Wang, Y. (2012) Neurodegeneration-associated TDP-43 interacts with fragile X mental retardation protein (FMRP)/Staufen (STAU1) and regulates SIRT1 expression in neuronal cells, *The Journal of biological chemistry 287*, 22560-22572.

[54] Shinozaki, S., Chang, K., Sakai, M., Shimizu, N., Yamada, M., Tanaka, T., Nakazawa, H., Ichinose, F., Yamada, Y., Ishigami, A., Ito, H., Ouchi, Y., Starr, M. E., Saito, H., Shimokado, K., Stamler, J. S., and Kaneki, M. (2014) Inflammatory stimuli induce inhibitory S-nitrosylation of the deacetylase SIRT1 to increase acetylation and activation of p53 and p65, *Science signaling 7*, ra106.

[55] Qiu, G., Li, X., Che, X., Wei, C., He, S., Lu, J., Jia, Z., Pang, K., and Fan, L. (2015) SIRT1 is a regulator of autophagy: Implications in gastric cancer progression and treatment, *FEBS letters 589*, 2034-2042.

[56] Holland, D., Desikan, R. S., Dale, A. M., McEvoy, L. K., and Alzheimer's Disease Neuroimaging, I. (2012) Rates of decline in Alzheimer disease decrease with age, *PLoS One 7*, e42325.

[57] Murphy, M. P., and LeVine, H., 3rd. (2010) Alzheimer's disease and the amyloid-beta peptide, *J Alzheimers Dis 19*, 311-323.

[58] Novo, M., Freire, S., and Al-Soufi, W. (2018) Critical aggregation concentration for the formation of early Amyloid-beta (1-42) oligomers, *Sci Rep 8*, 1783.

[59] Sinha, S., and Lieberburg, I. (1999) Cellular mechanisms of beta-amyloid production and secretion, *Proc Natl Acad Sci U S A 96*, 11049-11053.

[60] Saido, T., and Leissring, M. A. (2012) Proteolytic degradation of amyloid beta-protein, *Cold Spring Harb Perspect Med 2*, a006379.

[61] Mosher, K. I., and Wyss-Coray, T. (2014) Microglial dysfunction in brain aging and Alzheimer's disease, *Biochemical pharmacology 88*, 594-604.

[62] Wu, Z., and Nakanishi, H. (2015) Lessons from Microglia Aging for the Link between Inflammatory Bone Disorders and Alzheimer's Disease, *Journal of immunology research 2015*, 471342.

[63] Fuger, P., Hefendehl, J. K., Veeraraghavalu, K., Wendeln, A. C., Schlosser, C., Obermuller, U., Wegenast-Braun, B. M., Neher, J. J., Martus, P., Kohsaka, S., Thunemann, M., Feil, R., Sisodia, S. S., Skodras, A., and Jucker, M. (2017) Microglia turnover with aging and in an Alzheimer's model via long-term in vivo single-cell imaging, *Nature neuroscience*.

[64] Keene, C. D., Darvas, M., Kraemer, B., Liggitt, D., Sigurdson, C., and Ladiges, W. (2016) Neuropathological assessment and validation of mouse models for Alzheimer's disease: applying NIA-AA guidelines, *Pathobiol Aging Age Relat Dis 6*, 32397.

[65] Niraula, A., Sheridan, J. F., and Godbout, J. P. (2017) Microglia Priming with Aging and Stress, *Neuropsychopharmacology : official publication of the American College of Neuropsychopharmacology 42*, 318-333.

[66] Flowers, A., Bell-Temin, H., Jalloh, A., Stevens, S. M., Jr., and Bickford, P. C. (2017) Proteomic anaysis of aged microglia: shifts in transcription, bioenergetics, and nutrient response, *Journal of neuroinflammation 14*, 96.

[67] Olah, M., Patrick, E., Villani, A. C., Xu, J., White, C. C., Ryan, K. J., Piehowski, P., Kapasi, A., Nejad, P., Cimpean, M., Connor, S., Yung, C. J., Frangieh, M., McHenry, A., Elyaman, W., Petyuk, V., Schneider, J. A., Bennett, D. A., De Jager, P. L., and Bradshaw, E. M. (2018) A transcriptomic atlas of aged human microglia, *Nature communications 9*, 539.

[68] Orre, M., Kamphuis, W., Osborn, L. M., Melief, J., Kooijman, L., Huitinga, I., Klooster, J., Bossers, K., and Hol, E. M. (2014) Acute isolation and transcriptome characterization of cortical astrocytes and microglia from young and aged mice, *Neurobiology of aging 35*, 1-14.

[69] Holtman, I. R., Raj, D. D., Miller, J. A., Schaafsma, W., Yin, Z., Brouwer, N., Wes, P. D., Moller, T., Orre, M., Kamphuis, W., Hol, E. M., Boddeke, E. W., and Eggen, B. J. (2015) Induction of a common microglia gene expression signature by aging and neurodegenerative conditions: a co-expression meta-analysis, *Acta neuropathologica communications 3*, 31.

[70] Wehrspaun, C. C., Haerty, W., and Ponting, C. P. (2015) Microglia recapitulate a hematopoietic master regulator network in the aging human frontal cortex, *Neurobiology of aging 36*, 2443 e2449-2443 e2420.

[71] Galatro, T. F., Holtman, I. R., Lerario, A. M., Vainchtein, I. D., Brouwer, N., Sola, P. R., Veras, M. M., Pereira, T. F., Leite, R. E. P., Moller, T., Wes, P. D., Sogayar, M. C., Laman, J. D., den Dunnen, W., Pasqualucci, C. A., Oba-Shinjo, S. M., Boddeke, E., Marie, S. K. N., and Eggen, B. J. L. (2017) Transcriptomic analysis of purified human cortical microglia reveals age-associated changes, *Nature neuroscience 20*, 1162-1171.

[72] Sikora, E., Arendt, T., Bennett, M., and Narita, M. (2011) Impact of cellular senescence signature on ageing research, *Ageing research reviews 10*, 146-152.

[73] Chen, N. C., Partridge, A. T., Tuzer, F., Cohen, J., Nacarelli, T., Navas-Martin, S., Sell, C., Torres, C., and Martin-Garcia, J. (2018) Induction of a Senescence-Like Phenotype in Cultured Human Fetal Microglia During HIV-1 Infection, *The journals of gerontology. Series A, Biological sciences and medical sciences*.

[74] Zecca, L., Gallorini, M., Schunemann, V., Trautwein, A. X., Gerlach, M., Riederer, P., Vezzoni, P., and Tampellini, D. (2001) Iron, neuromelanin and ferritin content in the substantia nigra of normal subjects at different ages: consequences for iron storage and neurodegenerative processes, *J Neurochem 76*, 1766-1773.

[75] Alimbetov, D., Davis, T., Brook, A. J., Cox, L. S., Faragher, R. G., Nurgozhin, T., Zhumadilov, Z., and Kipling, D. (2016) Suppression of the senescence-associated secretory phenotype (SASP) in human fibroblasts using small molecule inhibitors of p38 MAP kinase and MK2, *Biogerontology 17*, 305-315.

[76] Pluquet, O., Pourtier, A., and Abbadie, C. (2015) The unfolded protein response and cellular senescence. A review in the theme: cellular mechanisms of endoplasmic reticulum stress signaling in health and disease, *American journal of physiology. Cell physiology 308*, C415-425.

[77] Wang, R., Yu, Z., Sunchu, B., Shoaf, J., Dang, I., Zhao, S., Caples, K., Bradley, L., Beaver, L. M., Ho, E., Lohr, C. V., and Perez, V. I. (2017) Rapamycin inhibits the secretory phenotype of senescent cells by a Nrf2-independent mechanism, *Aging cell 16*, 564-574.

[78] Rozemuller, J. M., Eikelenboom, P., and Stam, F. C. (1986) Role of microglia in plaque formation in senile dementia of the Alzheimer type. An immunohistochemical study, *Virchows Arch B Cell Pathol Incl Mol Pathol 51*, 247-254.

[79] Vandenabeele, P., and Fiers, W. (1991) Is amyloidogenesis during Alzheimer's disease due to an IL-1-/IL-6-mediated 'acute phase response' in the brain?, *Immunol Today 12*, 217-219.

[80] Li, J. T., and Zhang, Y. (2018) TREM2 regulates innate immunity in Alzheimer's disease, *J Neuroinflammation 15*, 107.

[81] Tejera, D., and Heneka, M. T. (2016) Microglia in Alzheimer's disease: the good, the bad and the ugly, *Curr Alzheimer Res 13*, 370-380.

[82] Maat-Schieman, M. L., Rozemuller, A. J., van Duinen, S. G., Haan, J., Eikelenboom, P., and Roos, R. A. (1994) Microglia in diffuse plaques in hereditary cerebral hemorrhage with amyloidosis (Dutch). An immunohistochemical study, *J Neuropathol Exp Neurol 53*, 483-491.

[83] Wright, A. L., Zinn, R., Hohensinn, B., Konen, L. M., Beynon, S. B., Tan, R. P., Clark, I. A., Abdipranoto, A., and Vissel, B. (2013) Neuroinflammation and neuronal loss precede Abeta plaque deposition in the hAPP-J20 mouse model of Alzheimer's disease, *PLoS One 8*, e59586.

[84] Meda, L., Cassatella, M. A., Szendrei, G. I., Otvos, L., Jr., Baron, P., Villalba, M., Ferrari, D., and Rossi, F. (1995) Activation of microglial cells by beta-amyloid protein and interferon-gamma, *Nature 374*, 647-650.

[85] Rodriguez, J. J., Witton, J., Olabarria, M., Noristani, H. N., and Verkhratsky, A. (2010) Increase in the density of resting microglia precedes neuritic plaque formation and microglial activation in a transgenic model of Alzheimer's disease, *Cell Death Dis 1*, e1.

[86] Spangenberg, E. E., Lee, R. J., Najafi, A. R., Rice, R. A., Elmore, M. R., Blurton-Jones, M., West, B. L., and Green, K. N. (2016) Eliminating microglia in Alzheimer's mice prevents neuronal loss without modulating amyloid-beta pathology, *Brain 139*, 1265-1281.

[87] Song, E. S., Rodgers, D. W., and Hersh, L. B. (2018) Insulin-degrading enzyme is not secreted from cultured cells, *Scientific reports 8*, 2335.

[88] Shimizu, E., Kawahara, K., Kajizono, M., Sawada, M., and Nakayama, H. (2008) IL-4-induced selective clearance of oligomeric beta-amyloid peptide(1-42) by rat primary type 2 microglia, *Journal of immunology 181*, 6503-6513.

[89] Son, S. M., Kang, S., Choi, H., and Mook-Jung, I. (2015) Statins induce insulin-degrading enzyme secretion from astrocytes via an autophagy-based unconventional secretory pathway, *Molecular neurodegeneration 10*, 56.

[90] Miners, J. S., Baig, S., Tayler, H., Kehoe, P. G., and Love, S. (2009) Neprilysin and insulin-degrading enzyme levels are increased in Alzheimer disease in relation to disease severity, *Journal of neuropathology and experimental neurology 68*, 902-914.

[91] Nalivaeva, N. N., Beckett, C., Belyaev, N. D., and Turner, A. J. (2012) Are amyloid-degrading enzymes viable therapeutic targets in Alzheimer's disease?, *Journal of neurochemistry 120 Suppl 1*, 167-185.

[92] Wang, S., Wang, R., Chen, L., Bennett, D. A., Dickson, D. W., and Wang, D. S. (2010) Expression and functional profiling of neprilysin, insulin-degrading enzyme, and endothelin-converting enzyme in prospectively studied elderly and Alzheimer's brain, *Journal of neurochemistry 115*, 47-57.

[93] Miners, J. S., Baig, S., Palmer, J., Palmer, L. E., Kehoe, P. G., and Love, S. (2008) Abeta-degrading enzymes in Alzheimer's disease, *Brain pathology 18*, 240-252.

[94] Caccamo, A., Oddo, S., Sugarman, M. C., Akbari, Y., and LaFerla, F. M. (2005) Age- and region-dependent alterations in Abeta-degrading enzymes: implications for Abeta-induced disorders, *Neurobiology of aging 26*, 645-654.

[95] Leissring, M. A., Farris, W., Chang, A. Y., Walsh, D. M., Wu, X., Sun, X., Frosch, M. P., and Selkoe, D. J. (2003) Enhanced proteolysis of beta-amyloid in APP transgenic mice prevents plaque formation, secondary pathology, and premature death, *Neuron 40*, 1087-1093.

[96] Pacheco-Quinto, J., Herdt, A., Eckman, C. B., and Eckman, E. A. (2013) Endothelin-converting enzymes and related metalloproteases in Alzheimer's disease, *J Alzheimers Dis 33 Suppl 1*, S101-110.

[97] Baranger, K., Khrestchatisky, M., and Rivera, S. (2016) MT5-MMP, just a new APP processing proteinase in Alzheimer's disease?, *J Neuroinflammation 13*, 167.

[98] Zhao, R., Hu, W., Tsai, J., Li, W., and Gan, W. B. (2017) Microglia limit the expansion of beta-amyloid plaques in a mouse model of Alzheimer's disease, *Molecular neurodegeneration 12*, 47.

[99] Kummer, M. P., Vogl, T., Axt, D., Griep, A., Vieira-Saecker, A., Jessen, F., Gelpi, E., Roth, J., and Heneka, M. T. (2012) Mrp14 deficiency ameliorates amyloid beta burden by increasing microglial phagocytosis and modulation of amyloid precursor protein processing, *J Neurosci 32*, 17824-17829.

[100] Kong, Q., Peterson, T. S., Baker, O., Stanley, E., Camden, J., Seye, C. I., Erb, L., Simonyi, A., Wood, W. G., Sun, G. Y., and Weisman, G. A. (2009) Interleukin-1beta enhances nucleotide-induced and alpha-secretase-dependent amyloid precursor protein processing in rat primary cortical neurons via up-regulation of the P2Y(2) receptor, *J Neurochem 109*, 1300-1310.

[101] Buxbaum, J. D., Oishi, M., Chen, H. I., Pinkas-Kramarski, R., Jaffe, E. A., Gandy, S. E., and Greengard, P. (1992) Cholinergic agonists and interleukin 1 regulate processing and secretion of the Alzheimer beta/A4 amyloid protein precursor, *Proc Natl Acad Sci U S A 89*, 10075-10078.

[102] Prinzen, C., Muller, U., Endres, K., Fahrenholz, F., and Postina, R. (2005) Genomic structure and functional characterization of the human ADAM10 promoter, *FASEB journal : official publication of the Federation of American Societies for Experimental Biology 19*, 1522-1524.

[103] Hoey, S. E., Williams, R. J., and Perkinton, M. S. (2009) Synaptic NMDA receptor activation stimulates alpha-secretase amyloid precursor protein processing and inhibits amyloid-beta production, *J Neurosci 29*, 4442-4460.

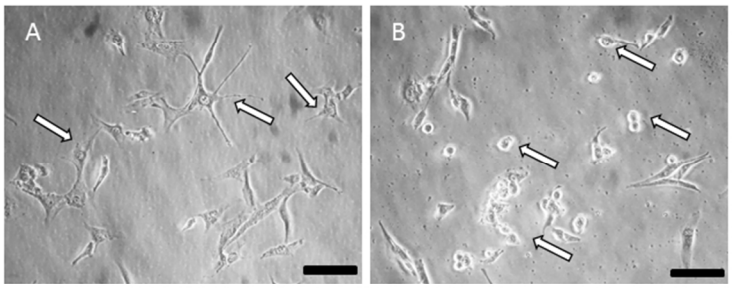

Figure 1

Figure 1

190x275mm (96 x 96 DPI)

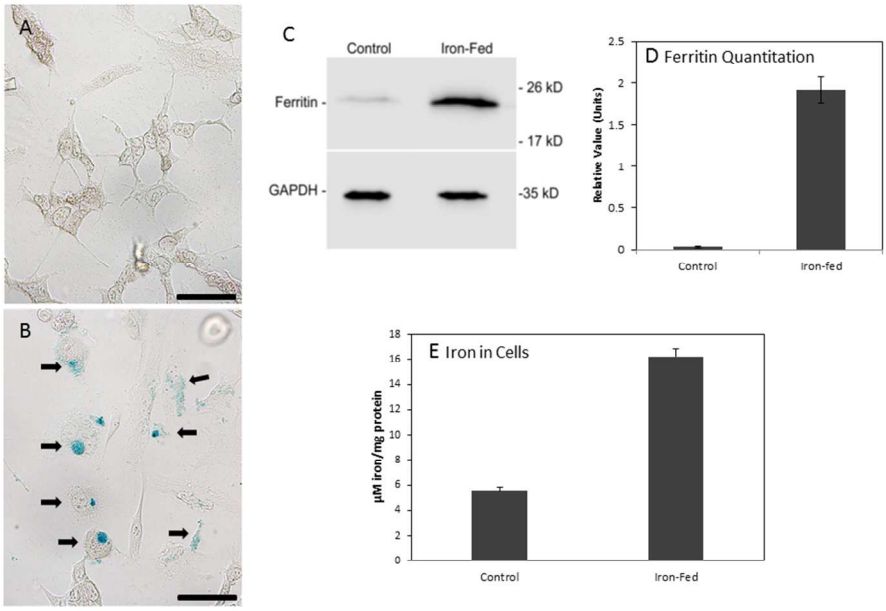

Figure 2

Figure 2

275x190mm (96 x 96 DPI)

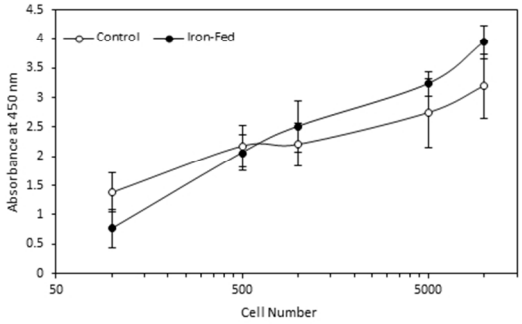

Figure 3

Figure 3

190x275mm (96 x 96 DPI)

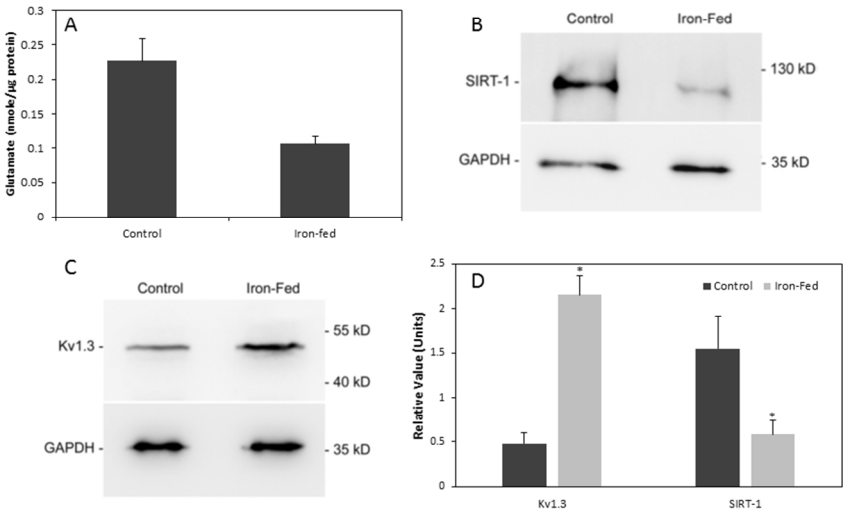

Figure 4

Figure 4

275x190mm (96 x 96 DPI)

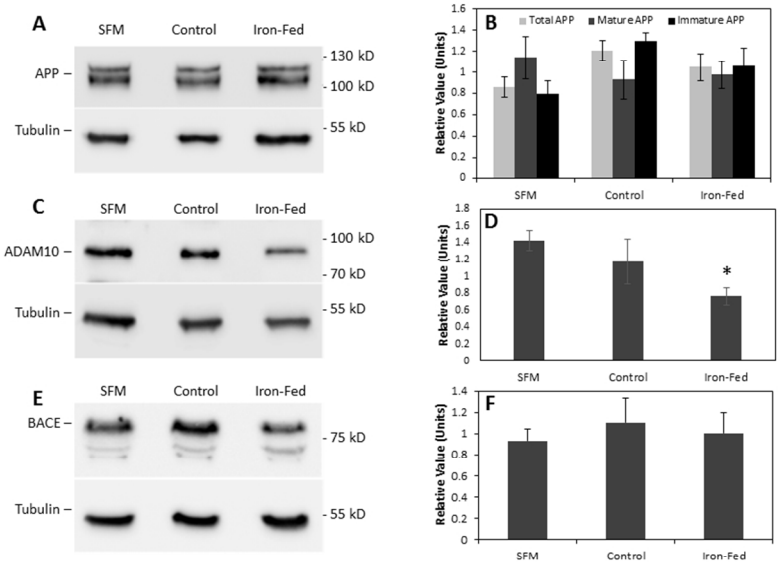

Figure 5

Figure 5

275x190mm (96 x 96 DPI)

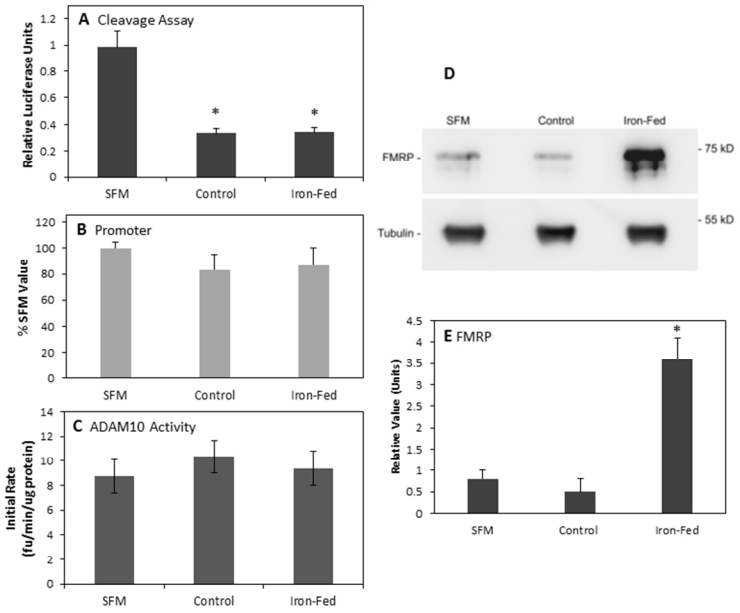

Figure 6

Figure 6

275x190mm (96 x 96 DPI)

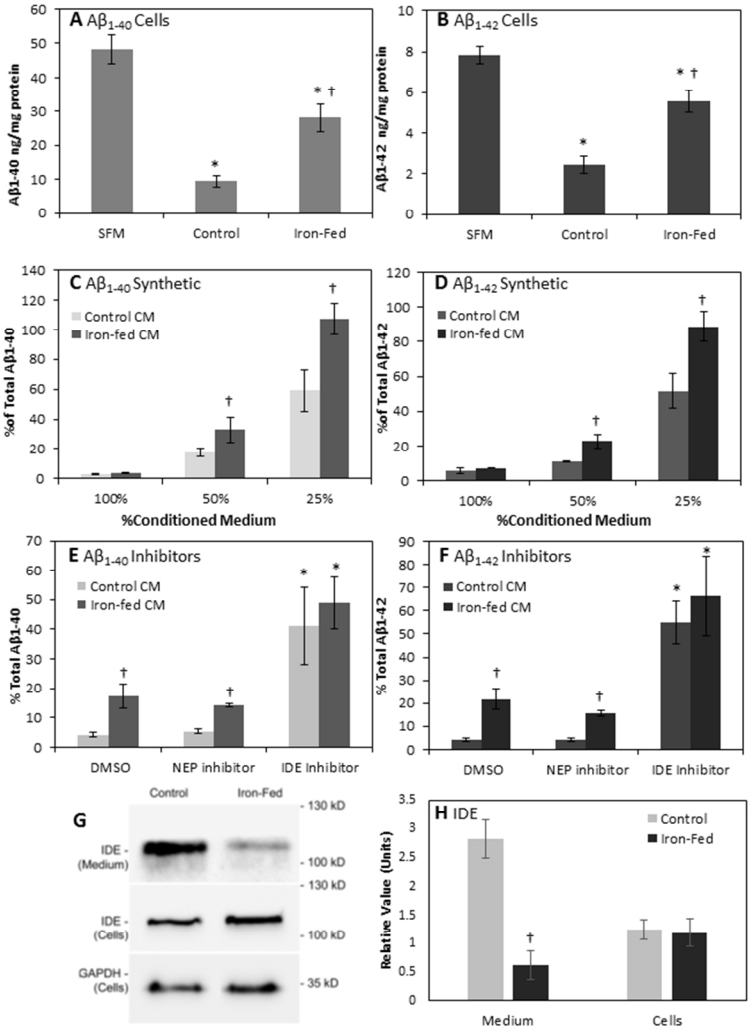

Figure 7

Figure 7

190x275mm (96 x 96 DPI)

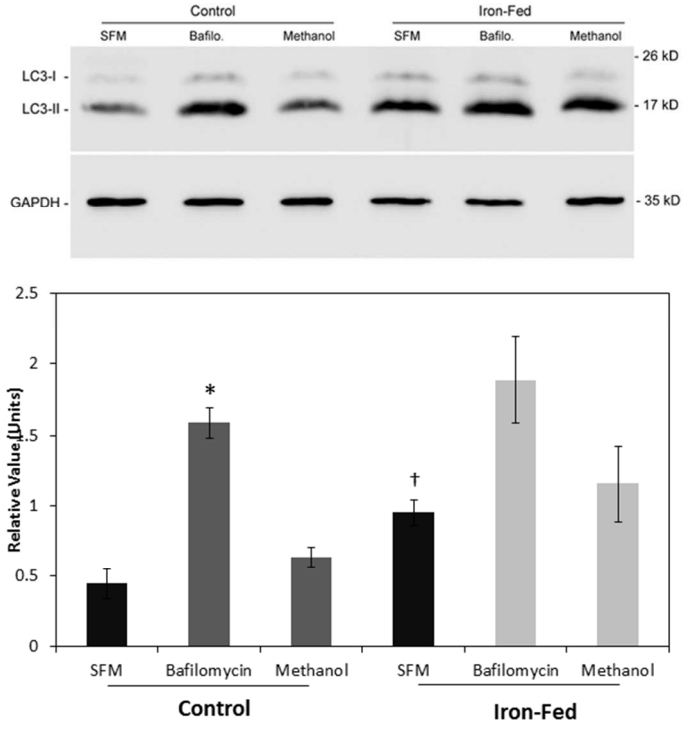

Figure 8

Figure 8

190x275mm (96 x 96 DPI)

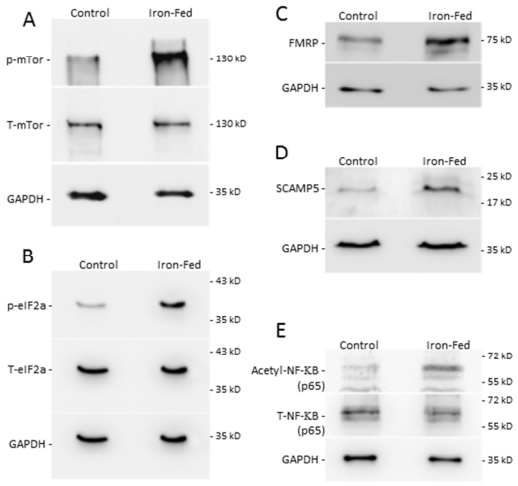

Figure 9

Figure 9

275x190mm (96 x 96 DPI)

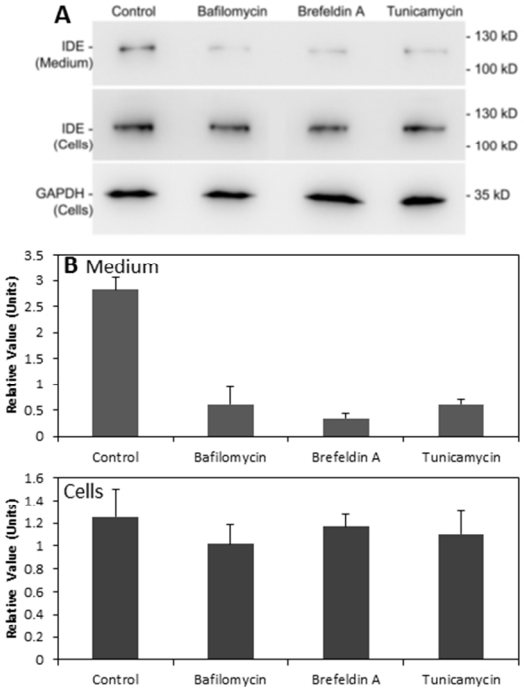

Figure 10

Figure 10

190x275mm (96 x 96 DPI)

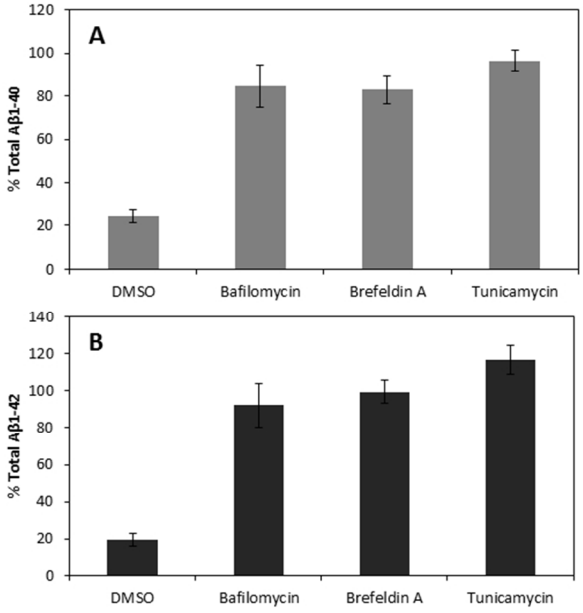

Figure 11

Figure 11

190x275mm (96 x 96 DPI)

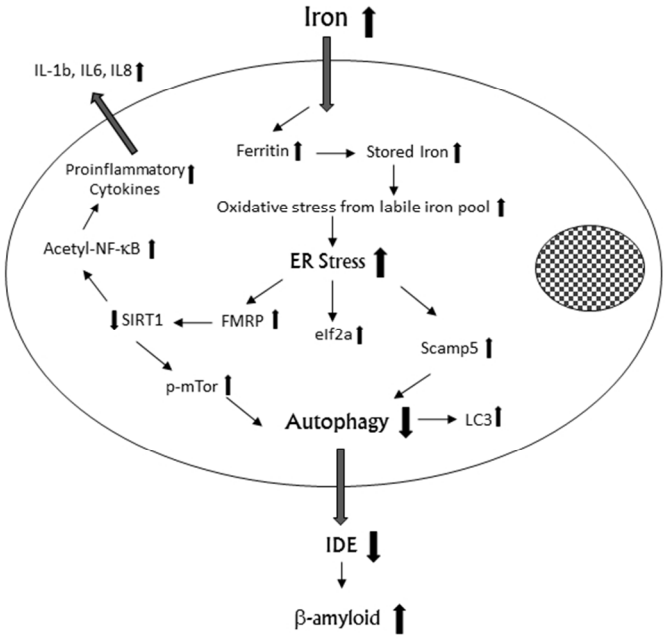

Figure 12

Figure 12

190x275mm (96 x 96 DPI)

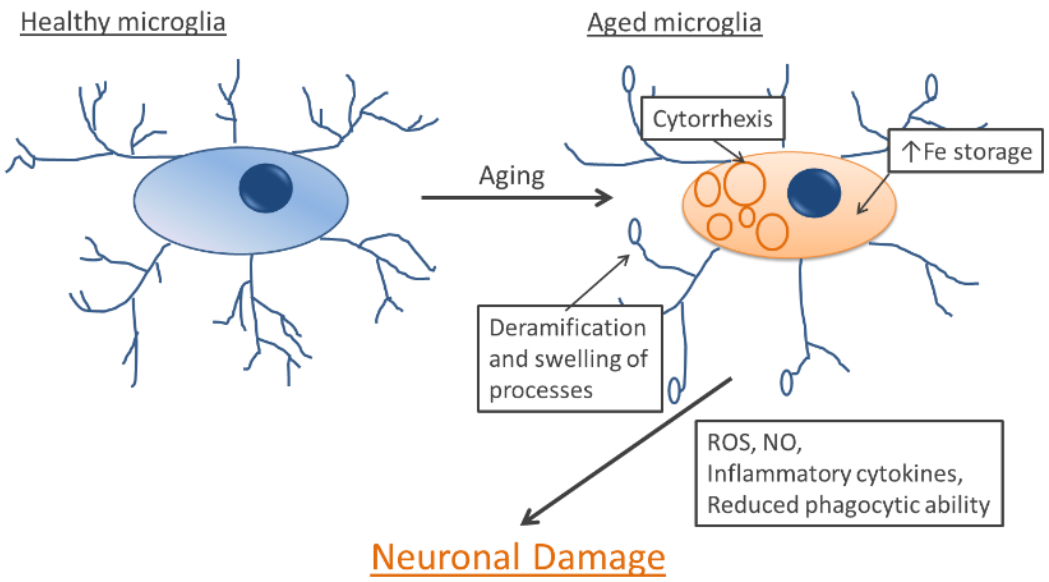
Healthy microglia
Aged microglia
Aging
Cytorrhexis
↑Fe storage
Deramification and swelling of processes
ROS, NO, Inflammatory cytokines, Reduced phagocytic ability
Neuronal Damage